Check for updates

Functionalization of graphene nanostructures with inorganic nanoparticles and their use for the removal of pharmaceutical pollutants in water

Jana Oliveras[1], Lionel Marcon[2], Neus G. Bastús[1]* and Victor Puntes[1,3,4]*

[1]Institut Català de Nanociència i Nanotecnologia (ICN2), CSIC, The Barcelona Institute of Science and Technology (BIST), Barcelona, Spain, [2]Institut Lumière Matière-UMR CNRS 5306, UCBL, Villeurbanne, France, [3]Institució Catalana de Recerca i Estudis Avançats (ICREA), Barcelona, Spain, [4]Vall d'Hebron Institut de Recerca (VHIR), Barcelona, Spain

Emerging pollutants such as pharmaceuticals are of special concern because despite their low environmental concentration, their biological activity can be intense, and they should be prevented to reach uncontrolledly to the environment. A graphene-based hybrid material decorated with Fe_3O_4 and TiO_2 nanoparticles (NPs) has been prepared to effectively remove emerging pollutants as nonsteroidal anti-inflammatory drugs (NSAIDs) Ibuprofen and Diclofenac present in water at low environmental concentrations by a one-step functionalization process following a novel gentle and scalable surfactant depletion approach. Following this methodology, nanoparticles are progressively deprived of their original surfactant in the presence of graphene, leading to the formation of hybrid nanostructures composed of two different types of nanoparticles well dispersed over the graphene nanosheets. Ibuprofen and Diclofenac adsorption kinetics on the composites was investigated via UV-Vis spectroscopy. The as prepared hybrid material possesses high adsorption capacity, superparamagnetic properties, photocatalytic behavior, and good water dispersibility. Thanks to incorporating TiO_2 nanoparticles as in situ catalysts, the adsorption performance of composites is restored after use, which could be a promising recycling pathway for the adsorbents in wastewater treatments.

KEYWORDS

graphene, nanomagnetite, photocatalysis, remediation, pharmaceuticals

Introduction

Nanoremediation refers to the use of nanostructures for efficiently capturing and degrading pollutants in water and soils, being a new solution to address the challenge of cleaning and making water drinkable in a simple, affordable, and scalable manner (Karn et al., 2009).

Emerging pollutants, especially pharmaceutically active compounds, have become a concern when present in the environment despite their low concentration (Daughton and Ternes, 1999; Stackelberg et al., 2004; Shannon et al., 2008; Taheran et al., 2018). These compounds are inherently designed to interact with biological systems. They are usually excreted -to some extent-non-metabolized by humans and livestock (Kümmerer, 2001), directly to wastewater or in sludge, later used as fertilizer (Kümmerer and Kümmerer, 2008; Patel et al., 2019). Up to now, over 200 pharmaceutical products have been detected in freshwaters; the most commonly found are antibiotics, followed by painkillers, analgesics, and antidepressants (Wilkinson et al., 2022).

Within these pharmaceutically active compounds, non-steroidal anti-inflammatory drugs (NSAIDs) are of significant concern as highly persistent pollutants, threatening the wellbeing of living species (de Voogt et al., 2009). These compounds display a heightened ability to diffuse passively across biological membranes and increased persistence in aquatic environments (Zhou et al., 2009). Although environmental concentrations are relatively low -μg/L to g/L in seawaters (Ginebreda et al., 2010), and ng/L in ground and drinking waters (Godfrey et al., 2007). They can be transported to other compartments (e.g., air, soil), concentrate and metabolize into equally or even more toxic substances (Heckmann et al., 2007; Parolini and Binelli, 2012; Du et al., 2016). Ibuprofen (IBP) and Diclofenac (DCF) are especially critical among NSAIDs. (de Voogt et al., 2009). They are estimated to be consumed in several kilotons per year globally, and their consumption tends to increase, accompanied by wide usage and irresponsible disposal.

Although significant advances have been made, conventional treatment methods are still incapable enough of treating the persistency of these compounds (Khan et al., 2004; Suarez et al., 2009; Kaur et al., 2016). Thus, despite reducing the concentration of these pharmaceuticals, a necessity of posttreatment to remove them is needed (Langenhoff et al., 2013). Adsorption appears to be the most broadly feasible removal method because of its versatility, broad applicability and economic feasibility. Numerous adsorbents have been developed, such as activated carbon, nanocomposites, metal frameworks and polymeric porous materials (Ahmed, 2017; Mlunguza et al., 2019). However, they have the disadvantage of low adsorption capacity, difficult separation from water, and challenging reuse after adsorption. Alternatively, advanced oxidation processes (AOP) offer great potential to degrade and mineralize NSAIDs (Ternes et al., 2003; Feng et al., 2013; Kanakaraju et al., 2018; Villanueva-Rodríguez et al., 2019). However, they often produce metabolites that are more problematic than the initial compound. Therefore, developing a cost-efficient removal technique for NSAIDs from aqueous media with a high adsorption capacity, facile separation and easy regenerability is still not fully developed.

"Graphene and graphene oxide-based materials (GMs) have been considered promising adsorbents for environmental decontamination due to their high surface area (~2,630 $m^2 \cdot g^{-1}$), large delocalized pi (π) electrons, and tunable chemical properties (Ternes et al., 2003; Chandra et al., 2010; Zhu et al., 2010; Maliyekkal et al., 2013). However, GMs in solution pose an additional pollution risk because they cannot be fully separated due to their nanoscale dimensions (Chen et al., 2016) dimensions (de Voogt et al., 2009). Additionally, their functionalization with inorganic nanoparticles (NPs) exhibits other advantageous and often synergistic behaviour (Al-Khateeb et al., 2014). For example, adding magnetic NPs to graphitic structures allows for quickly removing the adsorbent materials from the treated waters (Chen et al., 2016; Gul et al., 2021) while the semiconductor NPs adsorbed in the GMs could provide new ways to degrade photocatalytically NSAIDs efficiently (Sun et al., 2011; Guerra et al., 2018). However, despite the great potential of GMs, there are few papers currently published in the literature reporting on the use of GMs for the removal of IBP and DCF, mainly graphene oxide and reduced graphene-oxid, and showing indeed a relatively low adsorption capacity (Mendez-Arriaga et al., 2008; Nam et al., 2015; Romeiro et al., 2018; Shan et al., 2018). Additionally, none includes the functionalization of the GMs with inorganic NPs. Therefore, developing graphene-based hybrid materials for NSAIDs adsorption requires new studies on this topic.

Functionalization of GMs with magnetic Fe_3O_4 NPs are based on *in situ* and *ex situ* strategies. A straightforward approach includes the growth of Fe_3O_4 NPs directly on the surface of GMs following chemical treatments, heating or electrodeposition (Shan et al., 2017; Hiew et al., 2019; Khalil et al., 2020) of precursors electrostatically absorbed at the surface of GMs (Yang et al., 2009; Chandra et al., 2010; Cong et al., 2010; Shen et al., 2010; Su et al., 2011). Alternatively, GM-Fe_3O_4 hybrid composites can be produced by *ex situ* assembly. In this process, Fe_3O_4 NPs are synthesized in advance and subsequently attached to the surface of GM *via* electrostatic or covalent interactions. (He et al., 2010; He and Gao, 2010; Li et al., 2011). Both approaches present appealing benefits but also significant limitations. While the direct formation of the NPs onto GMs is simple, and large amounts of Fe_3O_4 NPs can be immobilized, uncontrollable reactions over the GM surface lead to limited control of NPs morphology (size, shape). On the other hand, the attachment of pre-formed NPs to GM is a more complex procedure that typically involves chemical modifications of both components and interconnection. Although it allows for NP morphological control and finer loading adjustment, it may require tedious and complicated surface modification processes. Remarkably, neither of the synthetic approaches provides a straightforward production of Graphene–NP hybrid structures composed of different types of NPs.

In this work, we designed a novel graphene-based hybrid material decorated with Fe_3O_4 and TiO_2 NPs to effectively

remove IBP and DCF present at environmental concentrations. The adsorption kinetics of IBP and DCP by GM hybrid nanostructures, whose rates depend much on the type of compound analyzed, its concentration, and the adsorbent used, were investigated *via* UV-Vis spectroscopy (Tran et al., 2022). Note that water purification at low pollutant concentrations is often more challenging than at higher concentrations, where physical and chemical approaches can be efficiently applied if the water is not significantly polluted and still holds some life (Marcon et al., 2021).

The novelty of this work relies on two distinct aspects. First, the materials' preparation presents remarkable advantages concerning state-of-the-art functionalization strategies. Herein, easily scalable one-step reaction (slow reaction at room T, therefore no critical mass or temperature gradients during synthesis). Following a novel surfactant-depletion approach similar to the one developed for CNTs functionalization (Ventosa et al., 2020). Following this method, NPs are slowly deprived of their original surfactant layer in the presence of graphene, leading to the formation of hybrid nanostructures composed of different types of NPs well dispersed over the graphene nanosheets while avoiding NP-NP aggregation. The second novel aspect relies on the additivity of the obtained structures. Thus, beyond showing a high adsorption capacity and good water dispersibility, hybrid structures are also superparamagnetic at room temperature, which allows their quickly removed by using a magnet, and thanks to incorporating TiO2 NPs, they are photocatalysts, so the absorbed material can be degraded and the adsorption performance partially restored, which seems a promising regeneration strategy.

Experimentals

Materials

Iron III Chloride (FeCl$_3$ anhydrous, powder, ≥99.99% trace metals basis), Iron(II) chloride tetrahydrate [FeCl$_2$·4H$_2$O puriss. p.a., ≥99.0% (RT)], stored in a glovebox under inert conditions, Diclofenac (DCF) and Tetramethylammonium hydroxide solution (TMAOH), Sodium Hydroxide (NaOH), Hydrochloric Acid (HCl) and Hydrogen Peroxide (30v/v) where purchased from Sigma-Aldrich and. Float-A-Lyzer devices of .5–1 kDa were purchased from Spectrum Labs and used after activation with 10% Ethanol solution as described by the company. 4-Isobutyl-alpha-methylphenylacetic acid, 99% (Ibuprofen-IBP) was purchased from Alfa Aesar. Titanium Isopropoxide was purchased from Fluka. Graphene flakes were kindly donated by Arben Merkoçi group at ICN2. All chemicals were used as received without further purification. Distilled water passed through a Millipore system (ρ = 18.2 MΩ) was used in all experiments.

Synthesis of Fe$_3$O$_4$/graphene hybrids
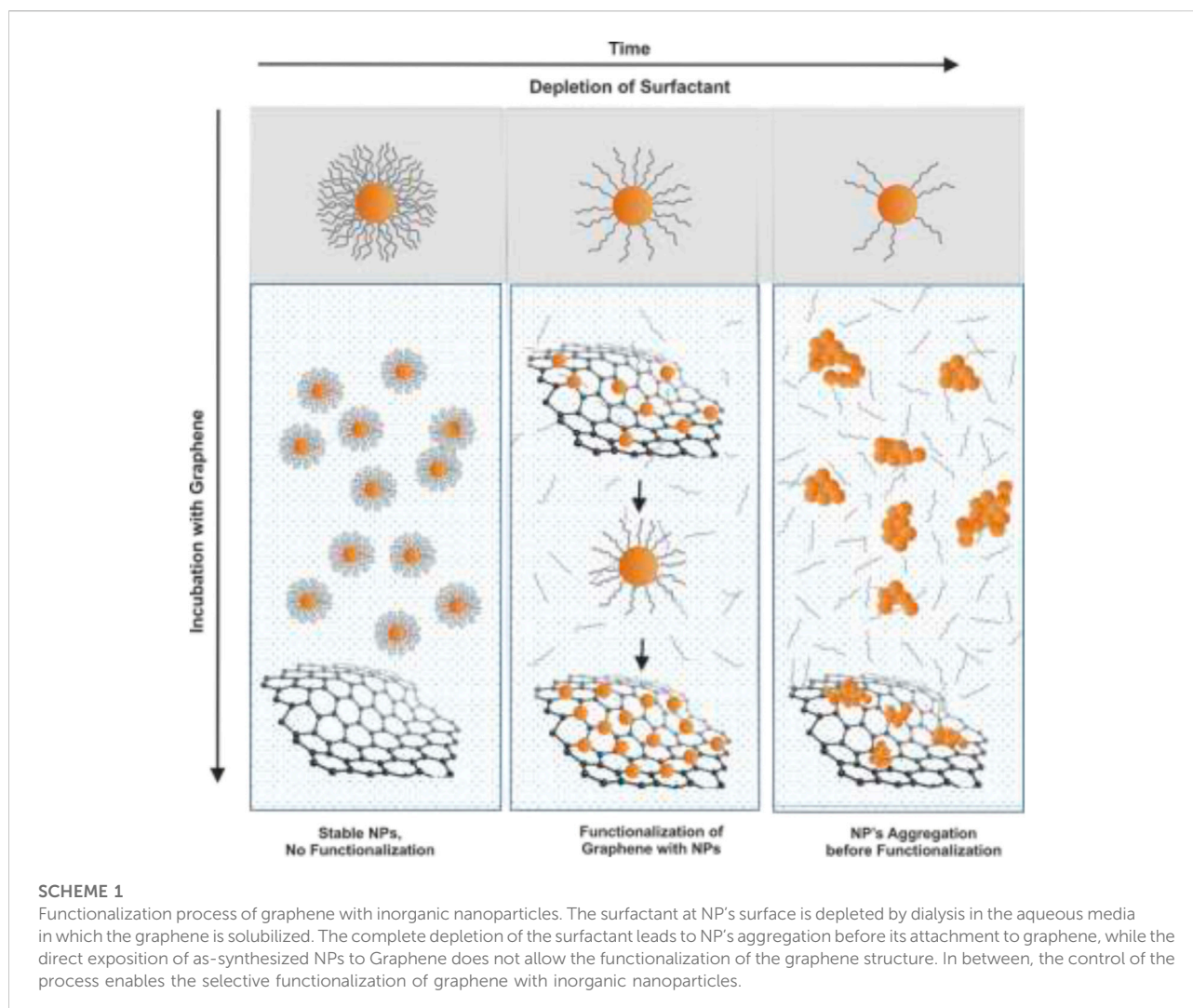
Synthesis of Fe$_3$O$_4$ NPs

Synthesis of Fe$_3$O$_4$ magnetite NPs of ~7 nm has been performed following a previously reported method. (He and Gao, 2010; Li et al., 2011). Briefly, in a 250 ml round bottom flask, 1.824 g of FeCl$_3$ anhydrous and .996 g of FeCl$_2$·4H$_2$O are sequentially added to 50 ml of mQ water deoxygenated under N$_2$ bubbling for 30 min and stirred until complete dissolution. Afterwards, 50 ml of 1 M TMAOH previously deoxygenated under N$_2$ bubbling for 30 min is poured continuously onto the solution containing the Fe(II) and Fe(III) precursors stirred at 600 rpm under Nitrogen atmosphere. The mixture is left stirring for 30 min. Once the reaction is completed the sample is washed twice by magnetically aided sedimentation and finally resuspended in 10 mM TMAOH. Sample is stored under nitrogen atmosphere to avoid its degradation.

Synthesis of TiO$_2$ NPs

Synthesis of TiO$_2$ anatase NPs of ~4 nm has been performed following a previously reported method. (Tran et al., 2022). Briefly, NaOH 3 M and HCl 3 M solutions were prepared. Afterwards, 2.07 ml of Titanium Isopropoxide were added to the 10 ml of the acid solution. Once the solution was homogeneous, 30 ml of mQ water and 5 ml of the base solution were carefully added to the solution containing the Titanium precursor, pH was then adjusted to pH 5. The solution was left covered in an oven at 70°C without stirring for 24 h. The resulting nanoparticles were centrifuged twice, the first time at 500 g and the second one at 1,000 g and resuspended in water. Afterwards, they were thoroughly sonicated in a sonics bath for several hours, centrifuged at 1,000 g and resuspended in 10 mM TMAOH.

Post-synthesis procedure, preparation of the hybrid

For the attachment of NPs to the graphene structure a calculated amount of 2·10^{12}NPs (see Supplementary Table S2 for calculations) were mixed with 625 μl of 5 mg/ml suspension of Graphene in H$_2$O (3.2·10^{12}NPs/mg graphene) and dialyzed versus H$_2$O in .5–1 kDa, 5 ml dialysis bags for 3 days, constantly stirred and renewing the dialysis water twice per day. After the procedure was completed, the dialyzed samples were precipitated under 2,000 g centrifugation for 10 min and the supernatant containing non-attached crystals was removed and replaced with 5 ml Milli-Q-Water, this process was performed twice. In the case of Fe$_3$O$_4$-TiO$_2$/Graphene hybrids, TiO$_2$ NPs were added to the dialysis bag after the afformentioned process was completed and decoration was accomplished by following the same steps. TiO$_2$ NPs were washed prior to dialysis *via* centrifugation and the pellet was re-suspended in water. Study of the deposition mechanism and the hybrid formation control was performed by synthesis of the hybrid at different and defined Graphene-to-Nanocrystal ratios. Concentrations of NPs were calculated by taking in account the size, composition and concentration of

SCHEME 1
Functionalization process of graphene with inorganic nanoparticles. The surfactant at NP's surface is depleted by dialysis in the aqueous media in which the graphene is solubilized. The complete depletion of the surfactant leads to NP's aggregation before its attachment to graphene, while the direct exposition of as-synthesized NPs to Graphene does not allow the functionalization of the graphene structure. In between, the control of the process enables the selective functionalization of graphene with inorganic nanoparticles.

precursors in the original synthesis, as well as its yield. This process was easily scalable and for the following experiments, 3.75 ml of Graphene suspension were used per each synthesis.

Synthesis of graphene oxide

Synthesis of graphene oxide was performed by adaptation of a simplified Hummer's method previously reported in the literature (Marcon et al., 2021). Briefly, .5 g of graphene flakes were mixed with 66.5 ml of H_2SO_4 in a 250 ml cooled by an ice bath. Afterward, 3 g of $KMnO_4$ were slowly added under vigorous stirring, at this point the solution was purplish green. Solution was left stirring for 3 and 6 days capped and it gradually turned to a deep green color. After this time had passed, the solution was poured in a 500 ml flask containing 66.5 ml of cold Mili-Q Water, this reaction was exothermic and effervescent and the solution turned to a reddish brown color. Finally, 4.5 ml of H_2O_2 were added and the solution was left stirring for 10 min, turning to a light yellow color. The final graphene oxide solution

was washed 3 times centrifuging at 10,000 g for 15 min and replacing the supernatant with 3 M HCl in order to remove the metal impurities that may had remained, finally the centrifugation process was repeated, replacing the supernatant with Mili-Q Water until the pH of the solution was 4-5.

Techniques

UV–Vis spectroscopy

UV–visible spectra were acquired with a Cary 60 spectrophotometer. Measurements were performed using a quartz cuvette with a 10 mm light pathway in the 200–800 nm range at room temperature.

Transmission electron microscopy

The morphology of the Fe_3O_4/Graphene hybrids were visualized using FEI Magellan 400L XHR SEM, in transmission
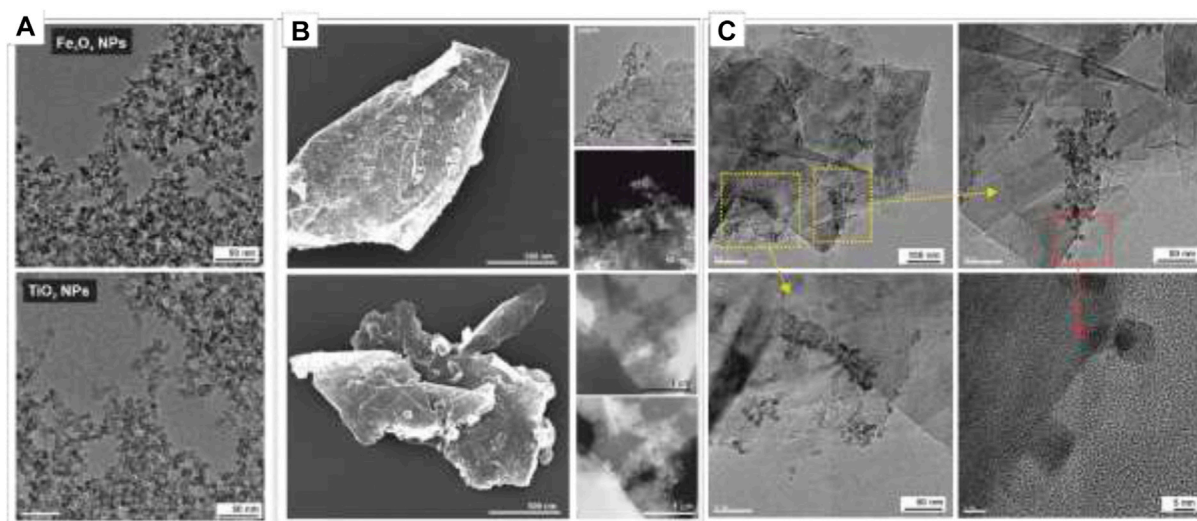
FIGURE 1
Representative Electron Microscopy Images of NPs and NPs/Graphene hybrids structures. **(A)** Transmission electron microscopy (TEM) images of as-synthetized Fe_3O_4 and TiO_2 NPs TEM. **(B)** Scanning Electron Microscopy (SEM), TEM and Scanning Transmission Electron Microscopy (STEM) taken with a high-angle annular dark field (HAADF) detector of $GM/Fe_3O_4/TiO_2$ hybrid nanostructures. **(C)** High-Resolution TEM (HRTEM) images of $GM/Fe_3O_4/TiO_2$.

mode operated at 20 kV. Morphology of Fe_3O_4NPs was observed using a FEI Tecnai G2 F20 HR(S)TEM operated at 200 kV in Bright Field mode. A droplet (10 µl) of the sample after 5 min ultrasonication of a 1:5 dilution of the samples was drop cast onto a piece of ultrathin carbon-coated 200-mesh copper grid (Ted-pella, Inc.) and left to dry in air.

SQUID measurements

The magnetic behaviour of the hybrid was evaluated *via* SQUID magnetometry and hysteresis loops observed at 10 K and 300 K.

Termogravimetric analysis (TGA)

For termogravimetric analysis was heated from 25°C to a final temperature of 900°C at a 10°C/min rate under an air flow of 24 ml/min.

Results and discussion

Rational of functionalization of GM with inorganic nanoparticles

The functionalization of graphene with inorganic NPs is based on the controlled destabilization of the NPs from their original surfactant layer, which typically provides stability. Under the appropriate conditions, the original surfactant layer of the NP is depleted in a controlled manner, while graphene act as a "surrogate ligand," trapping the partially surfactant-depleted NPs, leading to 2D

hybrid structures selectively decorated with NPs of controlled physicochemical features. This is achieved when low-binding surfactant stabilizers are employed. In these cases, there is a need for free surfactant in solution in equilibrium with the surfactant at the NP surface. So that if the free surfactant is removed, the NP surface is progressively stripped.

At short times, the direct exposition of as-synthesized NPs to GM does not result in the functionalization of the graphene structure. As time goes by and the surfactant is removed from the surface, NPs, are still stable against NP-NP aggregation but able to interact with the GM, resulting in GM decoration. On the contrary, fast depletion of the surfactant would lead to NPs aggregation in the solution prior to the adsorption onto the graphene in an aggregated form (Scheme 1). To control these conditions, the surfactant at the NP has to be in dynamic equilibrium with an excess of surfactant in the solution and then place the graphene-NP mix in a dialysis bag to promote slow surfactant depletion. The presented method is RT, straightforward, versatile, highly reproducible, recyclable, and scalable, thereby representing an exciting approach for the modular development of inorganic carbon-supported hybrid structures.

Synthesis and characterization of graphene oxide/Fe3O4/TiO2 hybrid nanostructures

Graphene (G, purity > 99%, layers < 3) was used as received without further purification. Highly monodisperse magnetite ~7 nm Fe_3O_4 NPs (1 mg NPs/ml) and ~7.5 nm TiO_2 NPs
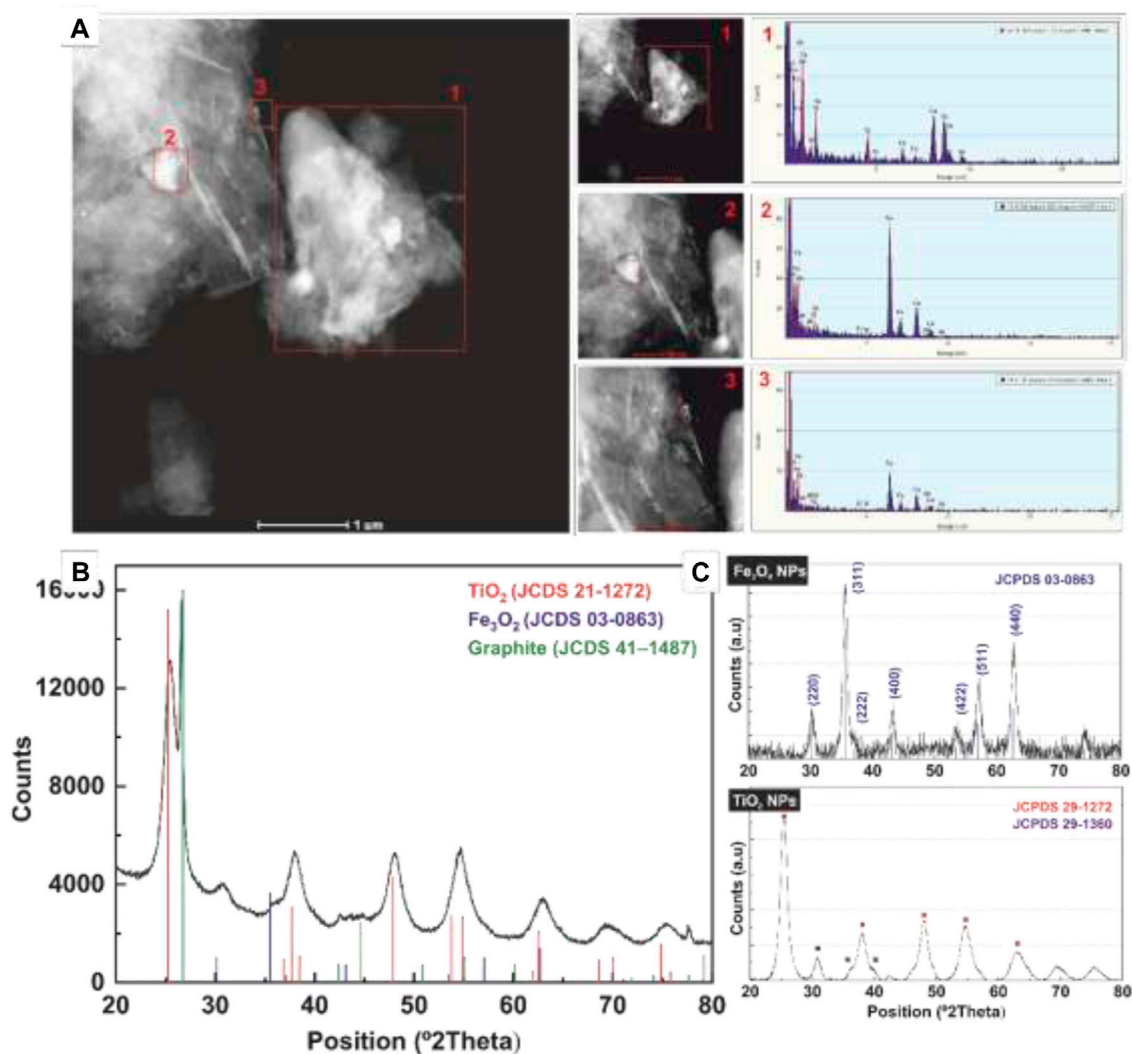
FIGURE 2
(A) EDS analysis of the Graphene/Fe3O4/TiO$_2$ hybrids structures. Scan profiles extracted from the representative sections of the HAADF-STEM images (as labelled) confirmed the presence of both types of NPs at the surface of the graphene sheet. The Cu peaks are the signal detected from the TEM grid. **(B)** XRD of Graphene/Fe$_3$O$_4$/TiO$_2$ structures. **(C)** XRD of Fe$_3$O$_4$ and TiO$_2$ NPs. **(A)** reveal the formation of highly uniform particles with well-defined morphologies. Structural characterization by X-ray diffraction (Supplementary Figure S1) shows well-defined peaks accordingly to the high crystallinity of the sample.

(1 mg NPs/ml) chemically stabilized with tetramethylammonium hydroxide (TMAOH) as surfactant were prepared following well-established synthetic procedures (Recillas et al., 2010; Casals et al., 2014). Representative transmission electron microscopy (TEM) images of as-obtained Fe$_3$O$_4$ NPs and TiO$_2$ NPs.

GM/Fe$_3$O$_4$/TiO$_2$ hybrid nanostructures were prepared by adding a known volume of Fe$_3$O$_4$ NPs (16 µl, 1 mg/ml, 3.2 10^{12} Fe$_3$O$_4$ NPs/1 mg graphene) to 1 ml of an aqueous solution of graphene (5 mg/ml) and left stirring for 3 days in a dialysis bag (6 cycles) against 5 L of H$_2$O. This process causes osmotic stress, which leads to the slow and progressive surface depletion of surfactant from the NP surface towards the counter-dialyzing solution. This process typically results in NP aggregation. However, adding the GM to the system results in the functionalization of the graphene sheets with NPs in a randomly distributed manner (Figure 1; Supplementary Figure S2). Once the NP is absorbed into the GM, the surfactant completely abandons the NP surface yielding NPs with a clean surface that directly attaches to the graphene, as observed by high-resolution TEM (Supplementary Figure S3). The resulting hybrids were purified, and a controlled volume of TiO$_2$ NPs (3.2 10^{12} TiO$_2$ NPs/1 mg graphene) was added to the aqueous
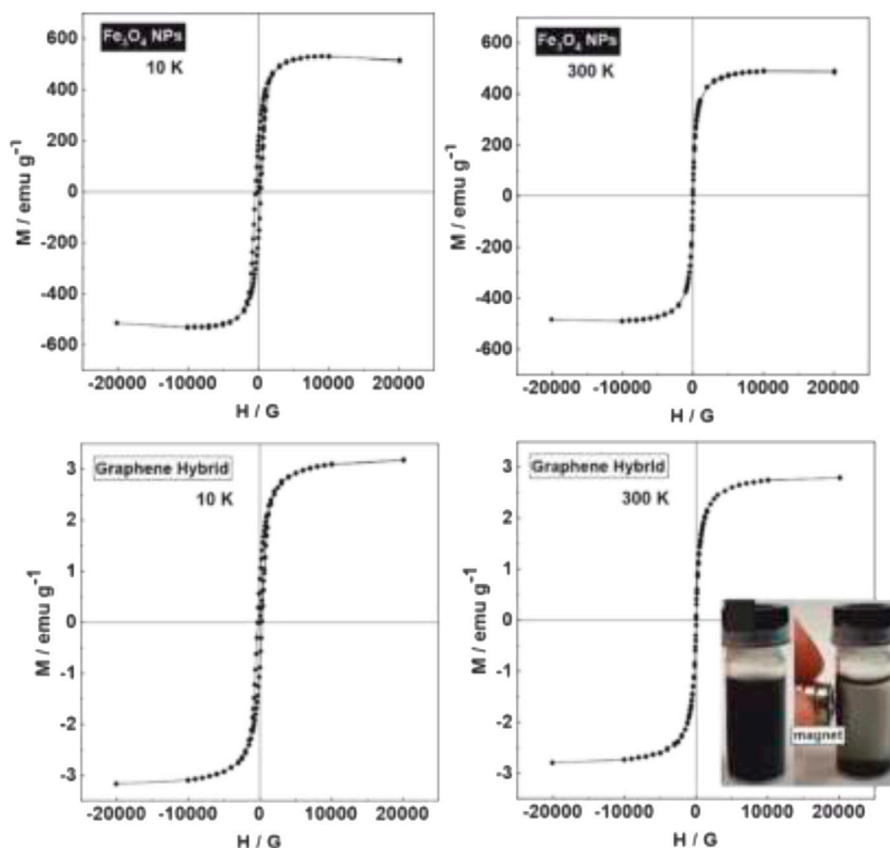
FIGURE 3
Magnetic behaviour of the graphene hybrid nanostructures dispersed in H$_2$O and its response to a permanent magnet. SQUID hysteresis loops from Fe$_3$O$_4$ NPs and graphene hybrids structures. Optical picture of distinctive coloured solutions from composite dispersed in H$_2$O and its response to a permanent magnet (Inset).
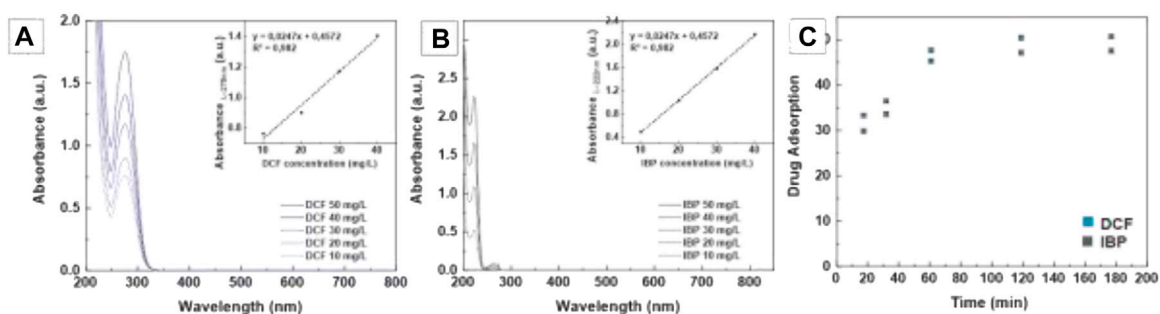

FIGURE 4
Calibration curves of IBP **(A)** and DFC **(B)** compounds. Time evolution experiment of Graphene Hybrids when exposed to different drugs **(C)**. Aliquots containing 1 g/L (3.2·10^{15} NPs/g graphene) Graphene hybrids were exposed to 100 mg/L and 68 mg/L for IBP and DCF solutions for different times. Adsorption was calculated from the abatement of the UV-Vis signal of the supernatant resulting from centrifuging the samples at 10,000 g for 10 min. DCF signal was monitored at 275 nm, while IBP signal was observed at the characteristic band at 222 nm and its temporary products at 264 nm.

graphene/Fe$_3$O$_4$ solution. Then, the above-described incubation process was repeated, yielding GM/Fe$_3$O$_4$/TiO$_2$ hybrid nanostructures. The robustness of the graphene hybrid final product was tested by ultra-sonication for up to 30 min without any observable change in morphology or NP detachment.

FIGURE 5
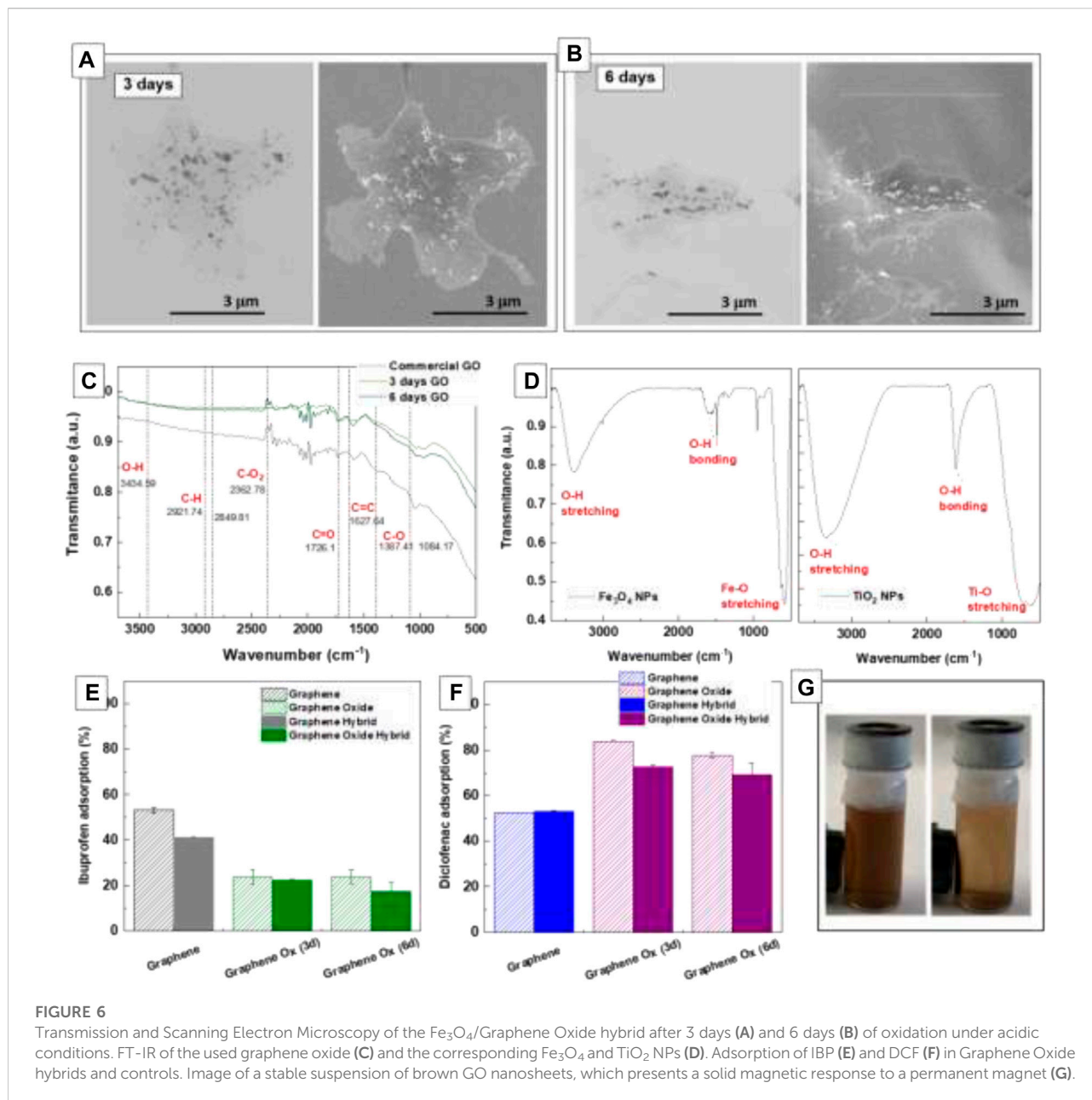Adsorption isotherms of Graphene and Graphene hybrids. Adsorption of IBP **(A)** and DCF solutions **(B)** at different drug concentrations exposed to Graphene/Fe_3O_4 hybrids ($3.2 \cdot 10^{15}$ NPs/g graphene; 1 g/L graphene). Adsorption of IBP **(C)** and DCF **(D)** (EC_{50} concentrations) exposed to varying concentrations of Graphene/Fe_3O_4 hybrids ($3.2 \cdot 10^{15}$ NPs/g Graphene) and Graphene.
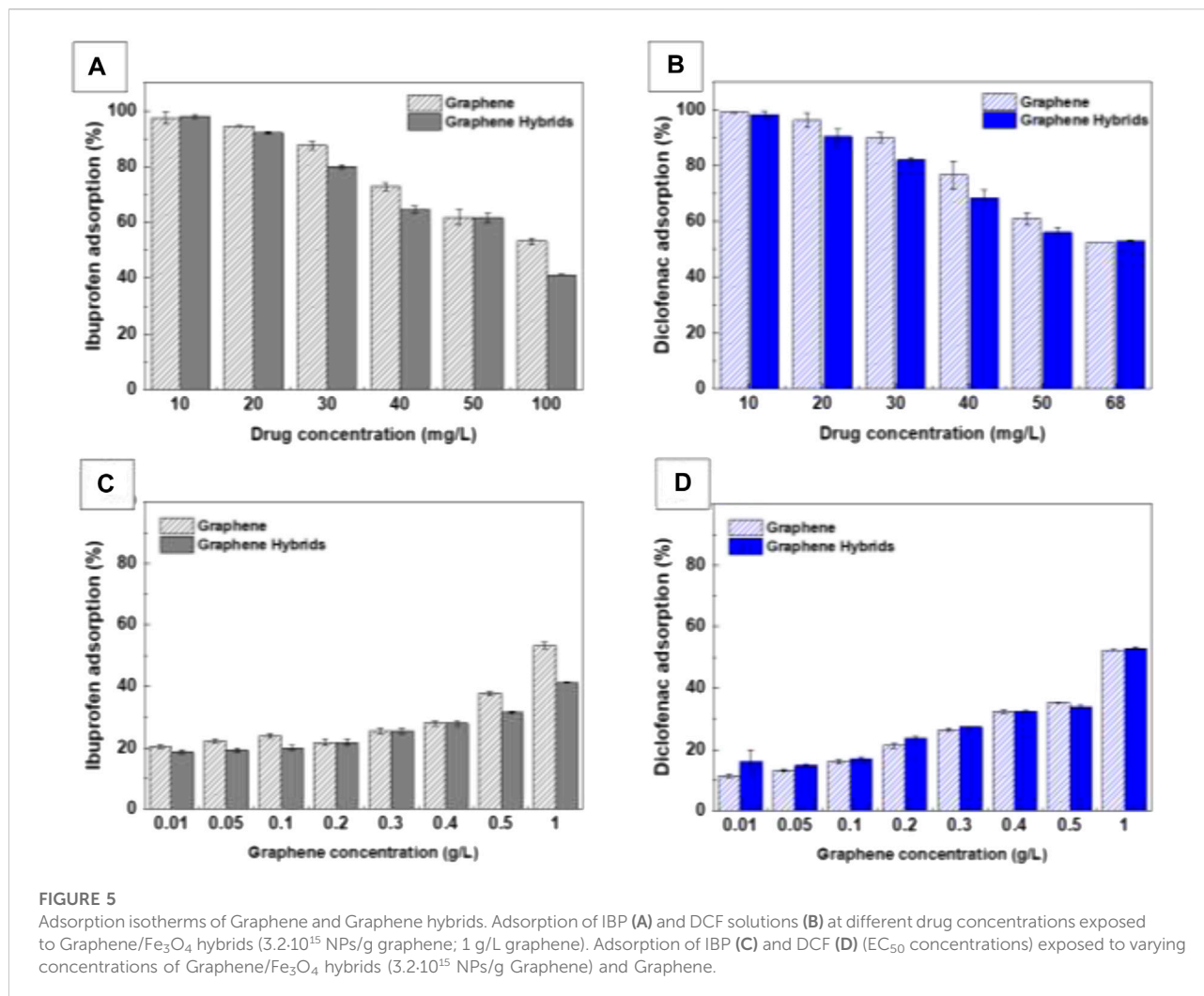
The morphology and structure of representative hybrids were investigated by scanning electron microscopy (SEM), high-angle annular dark-field scanning TEM (HAADF-STEM) and High-Resolution TEM (HR-TEM). SEM images reveal that NPs are uniformly attached on graphene sheets, which correlates with the bright spots in the HAADF-STEM images (Figure 1B). As is evident in the HR-TEM (Figure 1C), graphene is highly electron transparent, and the contrast here is due to three or more graphene layers. Results suggest that NPs are directly linked to the sheet, with no distance between the NPs and the graphene (Figure 1C).

The similar size and morphology of Fe_3O_4 NPs (~7 nm) and TiO_2 (~7.5 nm) make their discrimination difficult. Thus, the chemical composition analysis of the structure was assessed by Energy Dispersive X-Rays Spectroscopy (EDS) analysis (Figure 2A; Supplementary Figure S4), where scan profiles extracted from the representative sections of the HAADF-STEM images confirmed the presence of both types of NPs at the surface of the graphene sheet. In addition, the crystallographic structures of the graphene hybrid

nanostructures were also studied by XRD analysis (Figure 2B). The characteristic diffraction peak of graphite at 26o (JCPDS Card no. 41-1487) corresponding to the interplanar distance between graphene sheets (d = 0.345 nm) confirms that graphene substrate remained unaltered after the functionalization process. Furthermore, the most intense anatase TiO_2 peaks (JCPDS Card no. 21-1272) found at 24.8o, 37.3o, 47.6o, 53.5o, 55.1o, and 62.2o correspond to (101), (004), (200), (105), (211), and (204) crystal planes are similar to that of the free TiO_2 NPs. The diffraction spectrum also reveals the presence of Fe_3O_4 NPs. XRD patterns of the Fe_3O_4 and TiO_2 NPs and corresponding standard diffraction peaks of Fe_3O_4 (JCPDS card No. 03-0863) and TiO_2 (No. 29-1272 -anatase- and No. 29-1360 -brookite) are shown in Figure 2C. However, the iron fluorescence irradiated with X-ray from copper makes a much weaker signal, always hidden in the background of TiO_2 NPs, no matter how long is the acquisition time. In any case, the presence of significant Fe_3O_4 NPs can be observed in the magnetic response of the solution (Figure 3).

FIGURE 6
Transmission and Scanning Electron Microscopy of the Fe_3O_4/Graphene Oxide hybrid after 3 days **(A)** and 6 days **(B)** of oxidation under acidic conditions. FT-IR of the used graphene oxide **(C)** and the corresponding Fe_3O_4 and TiO_2 NPs **(D)**. Adsorption of IBP **(E)** and DCF **(F)** in Graphene Oxide hybrids and controls. Image of a stable suspension of brown GO nanosheets, which presents a solid magnetic response to a permanent magnet **(G)**.
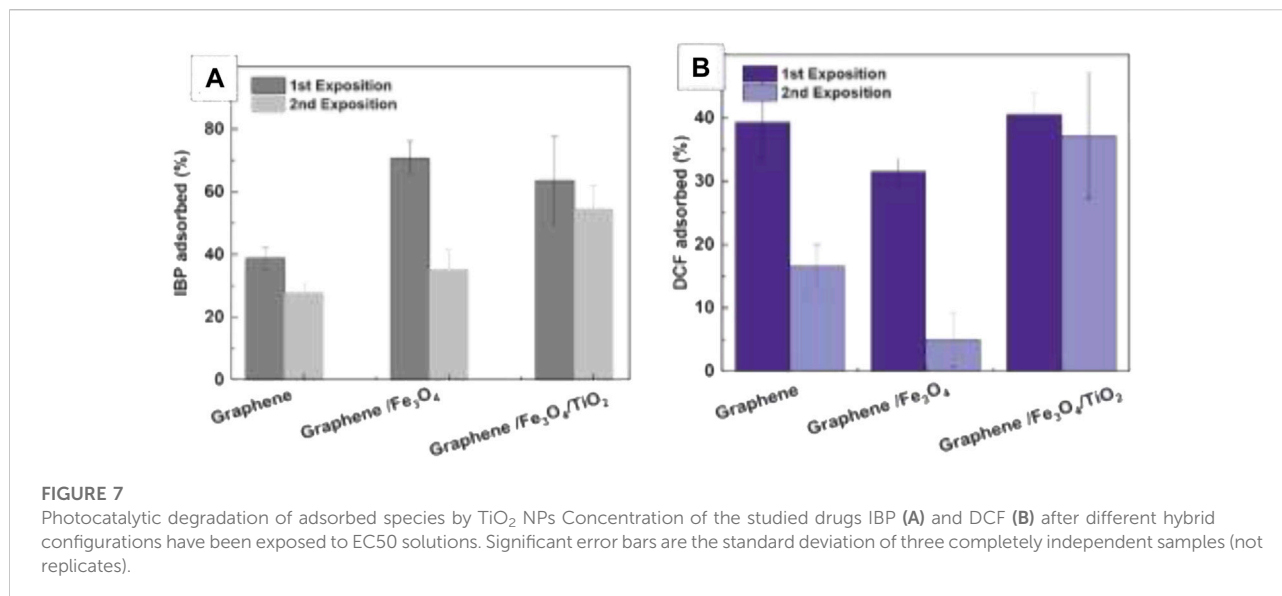
The two essential goals of this procedure are the magnetic and photocatalytic modification of the graphene sheet and the aqueous solubility of the final products. Figure 3 shows the solution response to a permanent magnet and its magnetic cleaning. The magnetic characteristics of the hybrid was assessed at 10 K and 300 K. While a small hysteresis is observed at low T, at RT, a canonical superparamagnetic behaviour with no hysteresis is observed, with a magnetic remanence of .5 the saturation magnetization, suggesting that NPs are well dispersed and non-aggregated. Interestingly, the magnetic properties are similar despite their absorption to the GM, indicating that the NPs have been individually added to the GM and not as aggregates. Otherwise, an increase in remanence and

hysteresis would appear due to interparticle dipolar interactions. Using as a reference the magnetic saturation value reported in the literature (Dar and Shivashankar, 2014), the weight percentage of Fe_3O_4 NPs was calculated to be around 4%, by which agrees with the measurements extracted from thermogravimetry analysis (Supplementary Figure S5).

Adsorption experiments

Several drug absorption experiments have been performed, exposing both graphene hybrids and plain

FIGURE 7
Photocatalytic degradation of adsorbed species by TiO$_2$ NPs Concentration of the studied drugs IBP **(A)** and DCF **(B)** after different hybrid configurations have been exposed to EC50 solutions. Significant error bars are the standard deviation of three completely independent samples (not replicates).

graphene as a control for further comparison. It is generally accepted that the adsorption process on GMs involves the combination of electrostatic and non-electrostatic interactions, including π–π electron donor-acceptor interactions and hydrophobic and electrostatic interactions (Nam et al., 2015; Jauris et al., 2016). IBP solutions were prepared in pH~6.3 Phosphate Buffer Solution (PBS) for optimal dissolution of the compound (Casals et al., 2014), while DCF was dissolved directly in Milli-Q water. UV-Vis was employed to analyze drug concentration after the proper calibrations (Figure 4). IBP signal was observed at the characteristic band at 222 nm (Dar and Shivashankar, 2014) (Figure 4A), and DCF signal was monitored at 275 nm (Recillas et al., 2010) (Figure 4B). The experiments were carried out in triplicate. The adsorption process has been observed mainly to occur in the first 80 min of exposure (Figure 4C). Samples were left for at least 2 h to ensure complete adsorption. Then, samples were purified magnetically to separate adsorbed from the non-adsorbed drug, and the supernatant was analyzed by UV-Vis spectroscopy. Purification by centrifugation yielded similar results, indicating that all graphene has been decorated with NPs.

In the first round of experiments, the drug concentration was set constant at the reported EC$_{50}$ -half of the drug concentration at which its maximum acute toxicity is observed-for sentinel aquatic species (*Daphnia Magna*), considered a standard in regulatory toxicology. (Cleuvers, 2004; Heckmann et al., 2007). These values are 100 mg/L for IBP and 68 mg/L for DCF in water, respectively. Graphene concentration was varied from .01 to 1 g/L. All final concentrations (Supplementary Table S1). In a second round, the concentration of graphene sheets was constant,

while drug concentration varied from 10–100 mg/L for IBP or 1–68 mg/L for DCF (Supplementary Table S2).

Adsorption experiments revealed a consistent dose-response behaviour (Figure 5). When the graphene hybrid concentration was fixed at 1 g/L (3.2·10^{15} NPs/g graphene), almost the complete removal of 10 mg/L of IBP (Figure 5A, in grey) or DCF (Figure 5B, in blue) was achieved. On the other hand, when the drug concentration was maintained at 100 mg/L IBP or 68 mg/L DCF, hybrids showed increased drug adsorption for increased concentrations of hybrids, as expected (Figures 5C, D). In both cases, the maximum adsorption capacity of the hybrid at the highest drug concentration tested is about 50%.

Bare graphene exposed to the drugs (Figure 5, striped patterns) showed slightly better adsorption rates than the hybrid counterparts, especially at high concentrations of drug and graphene. This fact could be attributed to the presence of NPs that block the adsorption sites of the graphene. To test this hypothesis, we studied the impact of NPs density on the drug adsorption by preparing graphene hybrids with different NP concentrations (0, 3.2·10^{14}, 3.2·10^{15}, 3.2·10^{16} NPs/g graphene; Graphene] = 1 g/L) and exposing them to 68 mg/L and 100 mg/L for DCF and IBP respectively solutions (see Supplementary Table S3). Obtained results (Supplementary Figure S6) suggest that variations in the concentration of NPs in the graphene hybrid do not significantly impact the adsorption of the tested drugs, indicating that the net surface area for drug adsorption of hybrids is comparable to that of unmodified graphene. Therefore, the minor variations in the adsorption observed values has been ascribed to differences in solubility, maybe due to the increased weight of NP-loaded graphene (Gutierrez et al., 2017; Talbot et al., 2021).

The absorption affinity onto graphene of organic molecules in water ultimately depends on charge distribution,

hydrophobicity and hydrophilicity. Therefore, we tested if more hydrophilic graphene oxide (GO) would be more or less soluble and absorb more or less drug. The same experiments were performed with GO synthesized *via* a modified Hummer's method: (Olumurewa et al., 2017): oxidation under acidic conditions at room temperature for 6 days. An aliquot was taken on the 3rd day of the experiment. Samples were thoroughly washed, concentrated at 1 g/L were characterized by Electron Microscopy and FT-IR, to confirm the oxidation of graphene.

Figures 6A, B shows a low magnification image of GO hybrid nanoestructures obtained after 3 days and 6 days. In both cases, the NPs can be resolved against the weak background of the GO sheet. Consistent with oxidation, FTIR spectrum of GO samples shows (Figure 6C) the characteristic vibration peaks allocated to O-H stretching, C=O stretching, and C-O stretching, which agrees well with commercial GO and previous works (RattanaChaiyakun et al., 2012; Hayyan et al., 2015). The broad peak at 3.434 cm^{-1} is assigned to OH groups and reveals the presence of hydroxy groups in GO. The band observed at 1.726 cm^{-1} is assigned to the carboxyl group, which would facilitate the attachment of NPs through electrostatic interaction (RattanaChaiyakun et al., 2012). The sharp peak found at 1.627 cm^{-1} corresponds to the stretching and bending vibration of OH groups of water molecules adsorbed on GO. The FT-IR spectrum of Fe$_3$O$_4$ and TiO$_2$ NPs shows the characteristic absorption bands around 3,450 cm^{-1} assigned to stretching and 1,630 cm^{-1} to bending vibration of O-H, representing the water as moisture. The intense peak around below 1,000 cm^{-1} is assigned to the Fe-O and Ti-O stretching bands. Finally, a stable suspension of brown GO nanosheets was obtained, which presents a solid magnetic response to a permanent magnet (Figure 6D, inset).

Adsorption of IBP and DCF in GO hybrids and controls are shown in Figures 6E–G. GO hybrid showed a notable decrease in adsorption when exposed to IBP and better results when exposed to DCF (Figures 6E,F). This fact appears relatively independent of oxidation time, 3d o 6d. Graphene is reported to interact *via* π-π with the benzoic ring of both species while, in the case of GO, other intermolecular forces are introduced to the system, such as hydrogen bridges. These new interactions would explain the improvement of results in the case of DCF, which has free electrons in its structure (from the Cl- and the NH- groups), while results from IBP, with only a polar group, are worse.

The final performance of the hybrids was testing the photocatalytic degradation of adsorbed species. Photocatalysis is considered an effective system for destroying many organics by generating non-selective and highly oxidative oxygen species, reducing considerably the organic load of effluents, using procedures with relatively low costs. Under UV light, highly photocatalytic TiO$_2$ NPs, with a bandgap of 3.2 eV, are activated, generating electron-

hole pairs that then reduce oxygen or oxidize water to produce very reactive free radical species (such as HO• and O2•−) that are responsible for molecule degradation. (Radjenović et al., 2009; Sousa et al., 2012; Sheng et al., 2013; Guo et al., 2016). Remarkably, compared to pure TiO$_2$ NPs, the light absorbance of GM/Fe$_3$O$_4$/TiO$_2$ hybrid nanostructures is extended into the visible range, which is in faithful agreement with the colour of the samples (i.e., white for bare TiO$_2$ NPs and dark grey for composite hybrid material).

To test the effects of photocatalysis on the exposed samples, we first incubated them for 2 h to the EC50 concentration of the studied drugs (100 mg/L and 68 mg/ml for the IBP and the DCF, respectively). Then, samples were purified magnetically and the supernatant was analyzed by UV-Vis spectroscopy (Figure 7, first exposition) and Then, samples were purified, exposed to UV light for 2 h, purified, and incubated again with drug solutions at the corresponding EC50 concentration. (Figure 7, second exposition). The obtained results indicated that, compared to controls, the loading capacity of GM/Fe$_3$O$_4$/TiO$_2$ hybrid nanostructures increased after the samples' re-exposure, indicating the destruction of drugs. Evidence in the literature and ongoing investigations suggest that optimising regeneration conditions can increase the reusability of the structures (Li et al., 2017; Gu et al., 2019).

Conclusion

In this work, we have reported the simple and straight forward preparation of graphene-based magnetic and optically active hybrid materials by the adsorption of magnetite and titania nanoparticles. They are intended for their application in removing and degrading (seek and destroy) emerging persistent organic pollutants as anti-inflammatory drugs—such as IBP and DCF. This materials are prepared by RT incubation of the NPs and the GM in surfactant depletion conditions. Modifications of the hybrid have been made, allowing us to understand 1) the role of the functional groups at the surface and the polarity of the adsorbed species in the case of the Graphene Oxide and 2) the additive properties that can offer a multi-modal hybrid in the case of the hybrid nanostructures. The presence of magnetite allow for the efficient removal of the hybrid while the presence of photocatalytic titania allow to degrade the absorbed drugs opening the door for recycling of the hybrid.

Data availability statement

The original contributions presented in the study are included in the article/Supplementary Material, further inquiries can be directed to the corresponding authors.

Author contributions

JO and LM performed the absorption experiments, JO and Neus bastus performed the NP synthesis and characterization, LM, NB, and VP designed the experiments and Neus Bastus and VP wrote the manuscript.

Funding

Acknowledgments

Conflict of interest

The authors declare that the research was conducted in the absence of any commercial or financial relationships that could be construed as a potential conflict of interest.

Publisher's note

All claims expressed in this article are solely those of the authors and do not necessarily represent those of their affiliated organizations, or those of the publisher, the editors and the reviewers. Any product that may be evaluated in this article, or claim that may be made by its manufacturer, is not guaranteed or endorsed by the publisher.

Supplementary material

The Supplementary Material for this article can be found online at: https://www.frontiersin.org/articles/10.3389/fceng.2022.1084035/full#supplementary-material

References

Ahmed, M. J. (2017). Adsorption of non-steroidal anti-inflammatory drugs from aqueous solution using activated carbons: Review. *J. Environ. Manag.* 190, 274–282. doi:10.1016/j.jenvman.2016.12.073

Al-Khateeb, L. A., Almotiry, S., and Salam, M. A. (2014). Adsorption of pharmaceutical pollutants onto graphene nanoplatelets. *Chem. Eng. J.* 248, 191–199. doi:10.1016/j.cej.2014.03.023

Casals, E., Barrena, R., Garcia, A., Gonzalez, E., Delgado, L., Busquets-Fite, M., et al. (2014). Programmed iron oxide nanoparticles disintegration in anaerobic digesters boosts biogas production. *Small* 10 (14), 2801–2808. doi:10.1002/smll.201303703

Chandra, V., Park, J., Chun, Y., Lee, J. W., Hwang, I. C., and Kim, K. S. (2010). Water-dispersible magnetite-reduced graphene oxide composites for arsenic removal. *ACS Nano* 4 (7), 3979–3986. doi:10.1021/nn1008897

Chen, L., Li, Y., Hu, S., Sun, J., Du, Q., Yang, X., et al. (2016). Removal of methylene blue from water by cellulose/graphene oxide fibres. *J. Exp. Nanosci.* 11 (14), 1156–1170. doi:10.1080/17458080.2016.1198499

Cleuvers, M. (2004). Mixture toxicity of the anti-inflammatory drugs diclofenac, ibuprofen, naproxen, and acetylsalicylic acid. *Ecotoxicol. Environ. Saf.* 59 (3), 309–315. doi:10.1016/s0147-6513(03)00141-6

Cong, H. P., He, J. J., Lu, Y., and Yu, S. H. (2010). Water-soluble magnetic-functionalized reduced graphene oxide sheets: *In situ* synthesis and magnetic resonance imaging applications. *Small* 6 (2), 169–173. doi:10.1002/smll.200901360

Dar, M. I., and Shivashankar, S. A. (2014). Single crystalline magnetite, maghemite, and hematite nanoparticles with rich coercivity. *RSC Adv.* 4 (8), 4105–4113. doi:10.1039/c3ra45457f

Daughton, C. G., and Ternes, T. A. (1999). Pharmaceuticals and personal care products in the environment: Agents of subtle change? *Environ. Health Perspect.* 107, 907–938. doi:10.1289/ehp.99107s6907

de Voogt, P., Janex-Habibi, M.-L., Sacher, F., Puijker, L., and Mons, M. (2009). Development of a common priority list of pharmaceuticals relevant for the water cycle. *Water Sci. Technol.* 59 (1), 39–46. doi:10.2166/wst.2009.764

Du, J., Mei, C. F., Ying, G. G., and Xu, M. Y. (2016). Toxicity thresholds for diclofenac, acetaminophen and ibuprofen in the water flea Daphnia magna.

Bull. Environ. Contam. Toxicol. 97 (1), 84–90. doi:10.1007/s00128-016-1806-7

Feng, L., van Hullebusch, E. D., Rodrigo, M. A., Esposito, G., and Oturan, M. A. (2013). Removal of residual anti-inflammatory and analgesic pharmaceuticals from aqueous systems by electrochemical advanced oxidation processes. A review. *Chem. Eng. J.* 228, 944–964. doi:10.1016/j.cej.2013.05.061

Ginebreda, A., Muñoz, I., de Alda, M. L., Brix, R., López-Doval, J., and Barceló, D. (2010). Environmental risk assessment of pharmaceuticals in rivers: Relationships between hazard indexes and aquatic macroinvertebrate diversity indexes in the Llobregat River (NE Spain). *Environ. Int.* 36 (2), 153–162. doi:10.1016/j.envint.2009.10.003

Godfrey, E., Woessner, W. W., and Benotti, M. J. (2007). Pharmaceuticals in on-site sewage effluent and ground water, Western Montana. *Ground Water* 45 (3), 263–271. doi:10.1111/j.1745-6584.2006.00288.x

Gu, Y., Yperman, J., Carleer, R., D'Haen, J., Maggen, J., Vanderheyden, S., et al. (2019). Adsorption and photocatalytic removal of Ibuprofen by activated carbon impregnated with TiO2 by UV–Vis monitoring. *Chemosphere* 217, 724–731. doi:10.1016/j.chemosphere.2018.11.068

Guerra, F. D., Attia, M. F., Whitehead, D. C., and Alexis, F. (2018). Nanotechnology for environmental remediation: Materials and applications. *Molecules* 23 (7), 1760. doi:10.3390/molecules23071760

Gul, A., Khaligh, N. G., and Julkapli, N. M. (2021). Surface modification of carbon-based nanoadsorbents for the advanced wastewater treatment. *J. Mol. Struct.* 1235, 130148. doi:10.1016/j.molstruc.2021.130148

Guo, J., Yuan, S., Jiang, W., Yue, H., Cui, Z., and Liang, B. (2016). Adsorption and photocatalytic degradation behaviors of rhodamine dyes on surface-fluorinated TiO2 under visible irradiation. *RSC Adv.* 6 (5), 4090–4100. doi:10.1039/c5ra14379a

Gutierrez, A. M., Dziubla, T. D., and Hilt, J. Z. (2017). Recent advances on iron oxide magnetic nanoparticles as sorbents of organic pollutants in water and wastewater treatment. *Rev. Environ. Health* 32 (1-2), 111–117. doi:10.1515/reveh-2016-0063

Hayyan, M., Abo-Hamad, A., AlSaadi, M. A., and Hashim, M. A. (2015). Functionalization of graphene using deep eutectic solvents. *Nanoscale Res. Lett.* 10 (1), 324. doi:10.1186/s11671-015-1004-2

He, F., Fan, J., Ma, D., Zhang, L., Leung, C., and Chan, H. L. (2010). The attachment of Fe3O4 nanoparticles to graphene oxide by covalent bonding. *Carbon* 48 (11), 3139–3144. doi:10.1016/j.carbon.2010.04.052

He, H., and Gao, C. (2010). Supraparamagnetic, conductive, and processable multifunctional graphene nanosheets coated with high-density Fe3O4 nanoparticles. *ACS Appl. Mat. Interfaces* 2 (11), 3201–3210. doi:10.1021/am100673g

Heckmann, L. H., Callaghan, A., Hooper, H. L., Connon, R., Hutchinson, T. H., Maund, S. J., et al. (2007). Chronic toxicity of ibuprofen to Daphnia magna: Effects on life history traits and population dynamics. *Toxicol. Lett.* 172 (3), 137–145. doi:10.1016/j.toxlet.2007.06.001

Hiew, B. Y. Z., Lee, L. Y., Lee, X. J., Gan, S., Thangalazhy-Gopakumar, S., Lim, S. S., et al. (2019). Adsorptive removal of diclofenac by graphene oxide: Optimization, equilibrium, kinetic and thermodynamic studies. *J. Taiwan Inst. Chem. Eng.* 98, 150–162. doi:10.1016/j.jtice.2018.07.034

Jauris, I. M., Matos, C. F., Saucier, C., Lima, E. C., Zarbin, A. J., Fagan, S. B., et al. (2016). Adsorption of sodium diclofenac on graphene: A combined experimental and theoretical study. *Phys. Chem. Chem. Phys.* 18 (3), 1526–1536. doi:10.1039/c5cp05940b

Kanakaraju, D., Glass, B. D., and Oelgemöller, M. (2018). Advanced oxidation process-mediated removal of pharmaceuticals from water: A review. *J. Environ. Manag.* 219, 189–207. doi:10.1016/j.jenvman.2018.04.103

Karn, B., Kuiken, T., and Otto, M. (2009). Nanotechnology and *in situ* remediation: A review of the benefits and potential risks. *Environ. Health Perspect.* 117 (12), 1813–1831. doi:10.1289/ehp.0900793

Kaur, A., Umar, A., and Kansal, S. K. (2016). Heterogeneous photocatalytic studies of analgesic and non-steroidal anti-inflammatory drugs. *Appl. Catal. A General* 510, 134–155. doi:10.1016/j.apcata.2015.11.008

Khalil, A. M. E., Memon, F. A., Tabish, T. A., Salmon, D., Zhang, S., and Butler, D. (2020). Nanostructured porous graphene for efficient removal of emerging contaminants (pharmaceuticals) from water. *Chem. Eng. J.* 398, 125440. doi:10.1016/j.cej.2020.125440

Khan, S. J., Wintgens, T., Sherman, P., Zaricky, J., and Schäfer, A. I. (2004). Removal of hormones and pharmaceuticals in the advanced water recycling demonstration plant in queensland, Australia. *Water Sci. Technol.* 50 (5), 15–22. doi:10.2166/wst.2004.0303

Kümmerer, K. (2001). Drugs in the environment: Emission of drugs, diagnostic aids and disinfectants into wastewater by hospitals in relation to other sources--a review. *Chemosphere* 45 (6-7), 957–969. doi:10.1016/s0045-6535(01)00144-8

Kümmerer, K. (2008). "Pharmaceuticals in the environment – a brief summary," in *Pharmaceuticals in the environment: Sources, fate, effects and risks*. Editor K. Kümmerer (Berlin, Heidelberg: Springer Berlin Heidelberg), 3–21.

Langenhoff, A., Inderfurth, N., Veuskens, T., Schraa, G., Blokland, M., Kujawa-Roeleveld, K., et al. (2013). Microbial removal of the pharmaceutical compounds ibuprofen and diclofenac from wastewater. *BioMed Res. Int.* 2013, 1–9. doi:10.1155/2013/325806

Li, C., Xu, Q., Xu, S., Zhang, X., Hou, X., and Wu, P. (2017). Synergy of adsorption and photosensitization of graphene oxide for improved removal of organic pollutants. *RSC Adv.* 7 (26), 16204–16209. doi:10.1039/c7ra01244f

Li, Y., Chu, J., Qi, J., and Li, X. (2011). An easy and novel approach for the decoration of graphene oxide by Fe3O4 nanoparticles. *Appl. Surf. Sci.* 257 (14), 6059–6062. doi:10.1016/j.apsusc.2011.01.127

Maliyekkal, S. M., Sreeprasad, T. S., Krishnan, D., Kouser, S., Mishra, A. K., Waghmare, U. V., et al. (2013). Graphene: A reusable substrate for unprecedented adsorption of pesticides. *Small* 9 (2), 273–283. doi:10.1002/smll.201201125

Marcon, L., Oliveras, J., and Puntes, V. F. (2021). *In situ* nanoremediation of soils and groundwaters from the nanoparticle's standpoint: A review. *Sci. Total Environ.* 791, 148324. doi:10.1016/j.scitotenv.2021.148324

Mendez-Arriaga, F., Esplugas, S., and Gimenez, J. (2008). Photocatalytic degradation of non-steroidal anti-inflammatory drugs with TiO2 and simulated solar irradiation. *Water Res.* 42 (3), 585–594. doi:10.1016/j.watres.2007.08.002

Mlunguza, N. Y., Ncube, S., Nokwethemba Mahlambi, P., Chimuka, L., and Madikizela, L. M. (2019). Adsorbents and removal strategies of non-steroidal anti-inflammatory drugs from contaminated water bodies. *J. Environ. Chem. Eng.* 7 (3), 103142. doi:10.1016/j.jece.2019.103142

Nam, S. W., Jung, C., Li, H., Yu, M., Flora, J. R., Boateng, L. K., et al. (2015). Adsorption characteristics of diclofenac and sulfamethoxazole to graphene oxide in aqueous solution. *Chemosphere* 136, 20–26. doi:10.1016/j.chemosphere.2015.03.061

Olumurewa, K. O., Olofinjana, B., Fasakin, O., Eleruja, M. A., and Ajayi, E. O. B. (2017). Characterization of high yield graphene oxide synthesized by simplified hummers method. *Graphene* 6 (4), 85–98. doi:10.4236/graphene.2017.64007

Parolini, M., and Binelli, A. (2012). Sub-lethal effects induced by a mixture of three non-steroidal anti-inflammatory drugs (NSAIDs) on the freshwater bivalve *Dreissena polymorpha*. *Ecotoxicology* 21 (2), 379–392. doi:10.1007/s10646-011-0799-6

Patel, M., Kumar, R., Kishor, K., Mlsna, T., Pittman, C. U., and Mohan, D. (2019). Pharmaceuticals of emerging concern in aquatic systems: Chemistry, occurrence, effects, and removal methods. *Chem. Rev.* 119 (6), 3510–3673. doi:10.1021/acs.chemrev.8b00299

Radjenović, J., Sirtori, C., Petrović, M., Barceló, D., and Malato, S. (2009). Solar photocatalytic degradation of persistent pharmaceuticals at pilot-scale: Kinetics and characterization of major intermediate products. *Appl. Catal. B Environ.* 89 (1), 255–264. doi:10.1016/j.apcatb.2009.02.013

Rattana, T., Chaiyakun, S., Witit-anun, N., Nuntawong, N., Chindaudom, P., Oaew, S., et al. (2012). Preparation and characterization of graphene oxide nanosheets. *Procedia Eng.* 32, 759–764. doi:10.1016/j.proeng.2012.02.009

Recillas, S., Garcia, A., Gonzalez, E., Casals, E., Puntes, V., Sanchez, A., et al. (2010). Use of CeO2, TiO2 and Fe3O4 nanoparticles for the removal of lead from water: Toxicity of nanoparticles and derived compounds. *Desalination* 277 (1-3), 213–220. doi:10.1016/j.desal.2011.04.036

Romeiro, A., Azenha, M. E., Canle, M., Rodrigues, V. H. N., Da Silva, J. P., and Burrows, H. D. (2018). Titanium dioxide nanoparticle photocatalysed degradation of ibuprofen and naproxen in water: Competing hydroxyl radical attack and oxidative decarboxylation by semiconductor holes. *Chemistryselect* 3 (39), 10915–10924. doi:10.1002/slct.201801953

Shan, D., Deng, S., Jiang, C., Chen, Y., Wang, B., Wang, Y., et al. (2018). Hydrophilic and strengthened 3D reduced graphene oxide/nano-Fe3O4 hybrid hydrogel for enhanced adsorption and catalytic oxidation of typical pharmaceuticals. *Environ. Sci. Nano* 5 (7), 1650–1660. doi:10.1039/c8en00422f

Shan, D., Deng, S., Li, J., Wang, H., He, C., Cagnetta, G., et al. (2017). Preparation of porous graphene oxide by chemically intercalating a rigid molecule for enhanced removal of typical pharmaceuticals. *Carbon* 119, 101–109. doi:10.1016/j.carbon.2017.04.021

Shannon, M. A., Bohn, P. W., Elimelech, M., Georgiadis, J. G., Mariñas, B. J., and Mayes, A. M. (2008). Science and technology for water purification in the coming decades. *Nature* 452 (7185), 301–310. doi:10.1038/nature06599

Shen, J., Hu, Y., Shi, M., Li, N., Ma, H., and Ye, M. (2010). One step synthesis of graphene Oxide–Magnetic nanoparticle composite. *J. Phys. Chem. C* 114 (3), 1498–1503. doi:10.1021/jp909756r

Sheng, H., Li, Q., Ma, W., Ji, H., Chen, C., and Zhao, J. (2013). Photocatalytic degradation of organic pollutants on surface anionized TiO2: Common effect of anions for high hole-availability by water. *Appl. Catal. B Environ.* 138-139, 212–218. doi:10.1016/j.apcatb.2013.03.001

Sousa, M. A., Gonçalves, C., Vilar, V. J. P., Boaventura, R. A. R., and Alpendurada, M. F. (2012). Suspended TiO2-assisted photocatalytic degradation of emerging contaminants in a municipal WWTP effluent using a solar pilot plant with CPCs. *Chem. Eng. J.* 198-199, 301–309. doi:10.1016/j.cej.2012.05.060

Stackelberg, P. E., Furlong, E. T., Meyer, M. T., Zaugg, S. D., Henderson, A. K., and Reissman, D. B. (2004). Persistence of pharmaceutical compounds and other organic wastewater contaminants in a conventional drinking-water-treatment plant. *Sci. Total Environ.* 329 (1-3), 99–113. doi:10.1016/j.scitotenv.2004.03.015

Su, J., Cao, M., Ren, L., and Hu, C. (2011). Fe3O4–Graphene nanocomposites with improved lithium storage and magnetism properties. *J. Phys. Chem. C* 115 (30), 14469–14477. doi:10.1021/jp201666s

Suarez, S., Lema, J. M., and Omil, F. (2009). Pre-treatment of hospital wastewater by coagulation-flocculation and flotation. *Bioresour. Technol.* 100 (7), 2138–2146. doi:10.1016/j.biortech.2008.11.015

Sun, H., Cao, L., and Lu, L. (2011). Magnetite/reduced graphene oxide nanocomposites: One step solvothermal synthesis and use as a novel platform for removal of dye pollutants. *Nano Res.* 4 (6), 550–562. doi:10.1007/s12274-011-0111-3

Taheran, M., Naghdi, M., Brar, S. K., Verma, M., and Surampalli, R. Y. (2018). Emerging contaminants: Here today, there tomorrow. *Environ. Nanotechnol. Monit. Manag.* 10, 122–126. doi:10.1016/j.enmm.2018.05.010

Talbot, D., Queiros Campos, J., Checa-Fernandez, B. L., Marins, J. A., Lomenech, C., Hurel, C., et al. (2021). Adsorption of organic dyes on magnetic iron oxide nanoparticles. Part I: Mechanisms and adsorption-induced nanoparticle agglomeration. *ACS Omega* 6 (29), 19086–19098. doi:10.1021/acsomega.1c02401

Ternes, T. A., Stuber, J., Herrmann, N., McDowell, D., Ried, A., Kampmann, M., et al. (2003). Ozonation: A tool for removal of pharmaceuticals, contrast media and musk fragrances from wastewater? *Water Res.* 37 (8), 1976–1982. doi:10.1016/s0043-1354(02)00570-5

Tran, B. T., Tran, T. N., Tran, A. M. T., Nguyen, G. C. D., and Nguyen, Q. T. T. (2022). Simultaneous determination of paracetamol, ibuprofen, and caffeine in tablets by molecular absorption spectroscopy combined with classical least square method. *Molecules* 27 (9), 2657. doi:10.3390/molecules27092657

Ventosa, M., Oliveras, J., Bastús, N. G., Gimbert-Suriñach, C., Puntes, V., and Llobet, A. (2020). Nanocrystal–molecular hybrids for the photocatalytic oxidation of water. *ACS Appl. Energy Mat.* 3 (10), 10008–10014. doi:10.1021/acsaem.0c01685

Villanueva-Rodríguez, M., Bello-Mendoza, R., Hernández-Ramírez, A., and Ruiz-Ruiz, E. J. (2019). Degradation of anti-inflammatory drugs in municipal wastewater by heterogeneous photocatalysis and electro-Fenton process. *Environ. Technol.* 40 (18), 2436–2445. doi:10.1080/09593330.2018.1442880

Wilkinson, J. L., Boxall, A. B. A., Kolpin, D. W., Leung, K. M. Y., Lai, R. W. S., and Galbán-Malagón, C. (2022). Pharmaceutical pollution of the world's rivers. *Proc. Natl. Acad. Sci.* 119 (8), e2113947119. doi:10.1073/pnas.2113947119

Yang, X., Zhang, X., Ma, Y., Huang, Y., Wang, Y., and Chen, Y. (2009). Superparamagnetic graphene oxide–Fe3O4 nanoparticles hybrid for controlled targeted drug carriers. *J. Mat. Chem.* 19 (18), 2710. doi:10.1039/b821416f

Zhou, J. L., Zhang, Z. L., Banks, E., Grover, D., and Jiang, J. Q. (2009). Pharmaceutical residues in wastewater treatment works effluents and their impact on receiving river water. *J. Hazard. Mater.* 166 (2-3), 655–661. doi:10.1016/j.jhazmat.2008.11.070

Zhu, Y., Murali, S., Cai, W., Li, X., Suk, J. W., Potts, J. R., et al. (2010). Graphene and graphene oxide: Synthesis, properties, and applications. *Adv. Mat.* 22 (35), 3906–3924. doi:10.1002/adma.201001068